Tuvalu, PACC, SPREP

Chapter 1
Introduction to the Country Reports

1.1 Climate Summary

A climate summary is presented at the beginning of each country chapter which gives an overview of the observations and projections for the relevant country.

1.2 Data Availability

This section provides updated information on the meteorological observation networks and data records available in each country. The length, completeness and quality of historical data records differ from country to country. For many observation sites there have been changes in station position, instrumentation and local environment that have produced inhomogeneities which are artificial changes in the data over time. For rainfall, only records or parts of records that have passed homogeneity tests are used in this report. For temperature, where possible, inhomogeneities have been identified and corrected using statistical techniques. Details on the quality control and homogenisation procedures are available in Whan et al. (2013), and McGree et al. (2013) for temperature and rainfall respectively.

1.3 Seasonal Cycles

Information on temperature and rainfall seasonal cycles can be found in Australian Bureau of Meteorology and CSIRO (2011).

1.3.1 Wind-driven Waves

This section provides new information on wind-driven waves. Observational wave data in the Pacific are sparse, with few wave rider buoy records in the region. Continuous satellite altimeter coverage from 1993 exists, but the temporal and spatial characteristics of these data present a number of challenges on longer time scales, with insufficient data resolution or duration for long-term wave climate studies. To supplement observational data, so-called hindcasts are used. A hindcast is an estimate of past observational data from numerical models run for past years using historical forcing data. Hindcasts provide a homogenous dataset in both space and time for studying wave climate. A reanalysis is an assimilation of historical observational data, which may be used to drive a hindcast.

Historically, the ability to produce a hindcast has been limited by the lack of global high-resolution reanalysis wind data to force the wave model. The recently completed Climate Forecast System Reanalysis (CFSR; Saha et al., 2010), performed at the National Center for Environmental Prediction, provides hourly surface winds on a 0.3 degree spatial grid. These winds were used to force the WaveWatch III model (Tolman 1991, 2009) for the period 1979–2009. This hindcast comprised a global grid at a spatial resolution of 0.4 degrees, providing boundary data to high-resolution nested sub-grids of 10 and 4 arcminutes (18 and 7 km respectively) around Australia and Pacific Island Partner Countries (Figure 1.1). All output data were archived at hourly intervals. Data were taken from the nearest model grid point to locations of interest (e.g. capital cities) from the 4 arcminute grid.

1.3.2 Data Presented

The wave model outputs give information on ocean wave climate in terms of three main variables: Significant Wave Height (m), Mean Wave Period (s) and Mean Wave Direction (degrees clockwise from north, indicating the direction from which the wave is travelling) (see Table X.1 in each country report). A mean annual cycle for each variable was generated by finding the average of all values in each month.

For brevity, only wave height and direction are plotted, while values and confidence ranges are given for all three variables. These wave height values are for off-shore waves only and do not apply to any lagoonal waves in atolls, which are not modelled.
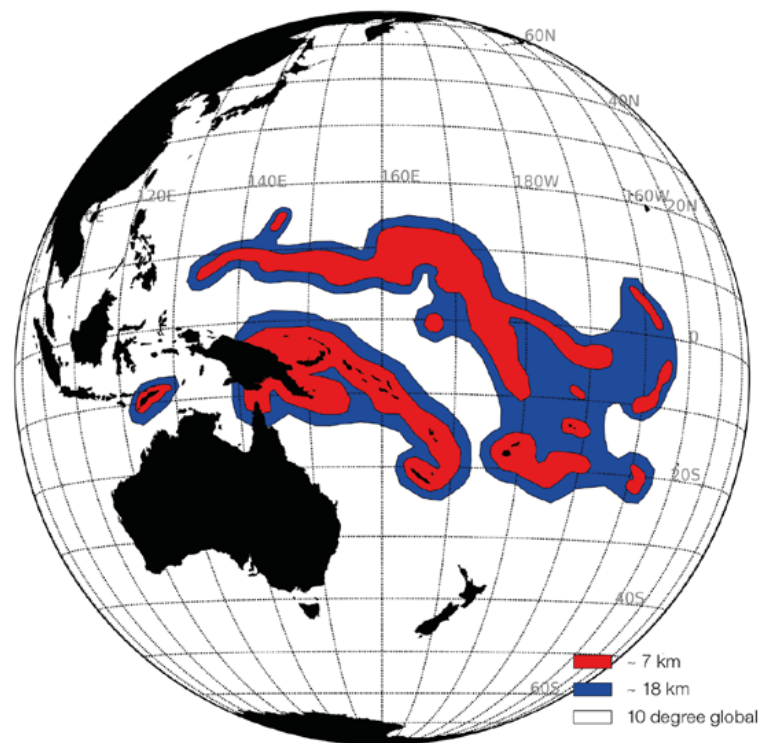

Figure 1.1: Region of validated high-resolution 30-year wave hindcast (an estimate of past observational data derived from models), showing a global 10 degree grid, with a series of nested grids of 10 and 4 arcminutes (~18 and 7 km respectively) in the western tropical Pacific. Data in 'Seasonal Cycles' sections for each country were taken from the nearest model grid point to locations of interest (e.g. capital cities) from the 4 arcminute (7km) grid.

Uncertainties are shown as a box drawn at 1 standard deviation from the mean, determined from all data in that month. Bars show the 5th and 95th percentiles, representing interannual variability.

1.4 Observed Trends

This section provides revised and updated analyses of observed trends for annual and seasonal air temperature and rainfall. Where only monthly records are available, these have been used to extend and fill gaps in the monthly average/total time series derived from daily values (subject to passing quality control and homogeneity checks). This product supersedes the Pacific Climate Change Science Programme (PCCSP), (Australian Bureau of Meteorology and CSIRO, 2011) high quality monthly rainfall and temperature datasets and related analyses. New analyses include trends in extreme air temperature, rainfall and ocean waves.

1.4.1 Annual, Half-year and Extreme (Daily) Air Temperature and Rainfall

Each chapter provides information on mean annual and half-year air temperature and total rainfall trends for one or two sites in each country, depending on data availability. Information is also provided on annual extreme (daily) air temperature and rainfall trends.

Linear trends for station records are calculated using a Kendall's tau-based slope estimator (Sen, 1968). This method has been widely used to compute trends in hydro-meteorological series (Wang and Swail, 2001; Zhang et al., 2005; Caesar et al., 2011). The significance of the trend and confidence intervals is modified to account for the presence of lag-1 autocorrelation in the residuals (Wang and Swail, 2001). Seventy percent of data are required (once processing has taken place) before a trend can be computed using the Kendall's slope estimator. Trends are deemed significant at the 5%

level when results lie beyond ±1.96 standard deviations of the median trend. In most cases, differences between the linear trends from this method and the ordinary least squares method (used in the mean and extreme plot in the Pacific Climate Change Data Portal www.bom. gov.au/climate/pccsp/) are small. Further information on methodology and additional results can be found in McGree et al. (2013) and Whan et al. (2013).

The eight rainfall and air temperature extreme indices (Table 1.1) used in the country chapters are based on the recommendations of the Expert Team on Climate Change Detection and Indices (ETCCDI, http://cccma.seos. univ.ca/ETCCDMI). Of the 27 core ETCCDI indices, 25 indices (excluding indices relating to freezing conditions) and several user-defined indices are available in the Pacific Climate Change Data Portal. Where the four air temperature extreme indices in Table 1.1 cannot be computed due to data limitations, four alternative but equally relevant indices (Table 1.2) have been presented.

Table 1.1: Selected rainfall and air temperature extreme indices.

Indices	Index ID	Definition	Units
Cool Nights	TN10p	Number of days with minimum temperature less than the 10th percentile for the base period 1971–2000	days/decade
Cool Days	TX10p	Number of days with maximum temperature less than the 10th percentile for the base period 1971–2000	days/decade
Warm Nights	TN90p	Number of days with minimum temperature greater than the 90th percentile for the base period 1971–2000	days/decade
Warm Days	TX90p	Number of days with maximum temperature greater than the 90th percentile for the base period 1971–2000	days/decade
Rain Days ≥ 1 mm	R1	Annual count of days where rainfall is greater or equal to 1 mm (0.039 inches)	days/decade
Very Wet Day Rainfall	R95p	Amount of rain where daily rainfall is greater than the 95th percentile for the reference period 1971–2000	mm/decade
Consecutive Dry Days	CDD	Maximum number of consecutive days with rainfall less than 1 mm (0.039 inches)	days/decade
Max 1-day Rainfall	Rx1day	Annual maximum 1-day rainfall	mm/decade

Table 1.2: Alternative air temperature extreme indices.

Indices	Index ID	Definition	Units
Max Tmax	TXx	Annual maximum value of daily maximum temperature	°C or F/decade
Max Tmin	TNx	Annual maximum value of daily minimum temperature	°C or F/decade
Min Tmax	TXn	Annual minimum value of daily maximum temperature	°C or F/decade
Min Tmin	TNn	Annual minimum value of daily minimum temperature	°C or F/decade

Colour-coding is used in data plots to show the influence of the El Niño–Southern Oscillation (ENSO): light-blue columns indicate El Niño years, dark blue columns La Niña years and grey columns neutral years. El Niño and La Niña years are defined using the June–December Southern Oscillation Index (SOI) calculated according to the standard Bureau of Meteorology method (www.bom.gov.au): a La Niña year is when the June–December SOI is greater than 5; an El Niño year is when June–December SOI is less than -5 (Power and Smith, 2007; Callaghan and Power, 2011). The influence of ENSO on the climate of the partner countries is not always clear. This is because: (1) these events often start in the middle of one year and continue into the next; (2) the impact of the ENSO on local rainfall and air temperature is not always simultaneous, i.e. there can be a lag of a few months between the ENSO development and impact at some locations; and (3) in some countries the ENSO does not have a major influence.

1.4.2 Tropical Cyclones

In each chapter, Section X.4.3, new information is presented on the number of tropical cyclones that have developed within or crossed Partner Country Exclusive Economic Zones (EEZs) between 1969/70–2010/11 seasons in the Southern Hemisphere, and 1977–2011 seasons in the Northern Hemisphere. Year to year changes in tropical cyclone occurrence are characterised by ENSO phases if the differences in average occurrence of tropical cyclones in El Niño and La Niña years, El Niño and neutral years and La Niña and neutral years are deemed statistically significant at the 5% level (using the method employed by Chand et al., 2013). Numbers of tropical cyclones crossing Southern Hemisphere Partner Country EEZs are obtained from the Pacific Tropical Cyclone Data Portal www.bom.gov.au/cyclone/history/tracks/. A 'preliminary' version of the equivalent for the Northern Hemisphere is available at http://reg.bom.gov.au/cyclone/

history/tracks/beta/?region=nw_pacific (Kuleshov et al., 2013).

Data for the Australian region (90°E–160°E) have been provided by the Australian Tropical Cyclone Warning Centres (Brisbane, Darwin and Perth), and for the eastern South Pacific Ocean (east of 160°E) by the meteorological services of Fiji and New Zealand. Tropical cyclone tracks from these archives were merged into one archive, ensuring consistency of track data when tropical cyclones cross regional borders. For the north-west Pacific, data have been obtained from the Regional Specialised Meteorological Centre, Tokyo. A graph with annual occurrences and an eleven-year running mean shows the interannual behaviour of tropical cyclones.

For most countries, the interannual variability in the number of tropical cyclones is large. For others, especially those close to the equator, only a small number of tropical cyclones occur within the EEZ boundary. One or other condition makes reliable detection of long-term trends in frequency difficult, and they are not calculated in this report. Intensity analysis is presented for the period 1981–2011 when tropical cyclone intensity estimates are most complete.

Some analysed tropical cyclone tracks include the tropical depression stage (sustained winds less than and equal to 34 knots) before and/or after tropical cyclone formation. This means that some 'tropical cyclones' may actually be tropical depressions when they developed within or passed through the Partner Country EEZ.

In addition, the area of cyclone genesis and tracks analysed for each Partner Country in this report (Australian Bureau of Meteorology and CSIRO, 2014), is different from the area analysed in Australian Bureau of Meteorology and CSIRO (2011). In the 2011 report, the area of analysis was restricted to tropical cyclones developing or crossing within a 400 km radius of a specific city within a Partner Country. In contrast, in this

report, the area of tropical cyclone genesis and tracks analysed is much larger, covering the entire EEZ of each Partner Country, and as a result the numbers of tropical cyclones given have increased for some countries.

1.5 Projections

1.5.1 Understanding climate model projections

New climate models

The country reports use global climate model (GCM) simulations taken from the international Coupled Model Intercomparison Project Phase 5 (CMIP5) (Taylor et al., 2012). These projections are an update of those produced using the Coupled Model Intercomparison Project Phase 3 (CMIP3) models presented in Australian Bureau of Meteorology and CSIRO (2011). Many CMIP5 models include components that were not in the CMIP3 models, including biogeochemistry and interactive aerosol. The core components of the models have also undergone some development. This means that some models can be used for new purposes, such as examining ocean chemistry reactions.

CMIP3 projections are still relevant and useful for impact and adaptation analyses. Many results from CMIP5 are similar to those from CMIP3, including *high confidence* in warming of the climate system, sea-level rise and an increase in rainfall along the equator (Australian Bureau of Meteorology and CSIRO, 2011). An important change to keep in mind is that the new projections are made using a new set of emissions scenarios (see New Emissions Scenarios). All model outputs should be used as a guide to what is plausible for a particular emissions scenario, not as a firm single 'prediction' of the future. In other words, projected changes (especially for the late 21st century) tend to vary strongly depending on what emissions scenario is used.

The CMIP5 dataset is still in development and will eventually contain outputs from more than 50 models. The performance of 27 CMIP5 models over the Pacific-Australia Climate Change Science and Adaptation Planning Program region was evaluated (Grose et al., 2014), leading to projections based on a maximum of 24 models for the South Pacific Convergence Zone (SPCZ) region, and 26 models in other regions. Models used in each analysis are listed in Appendix A (models not used for SPCZ countries are also listed).

Insights from the downscaling of previous CMIP3 models using the Conformal Cubic Atmospheric Model (CCAM) (McGregor, 2005) done for the Australian Bureau of Meteorology and CSIRO (2011) report are included throughout the country reports where relevant.

New Emissions Scenarios

Since it is uncertain how society and technology will evolve over the next century, it is impossible to know exactly how emissions of greenhouse gases and aerosols resulting from human activities will change in the future. Results in the country reports are presented for four new scenarios of greenhouse gases and aerosol emissions, called Representative Concentration Pathways (RCPs): RCP2.6 (very low emissions), RCP4.5 (low emissions), RCP6 (medium emissions) and RCP8.5 (very high emissions) used by the IPCC (2013). These cover a broader range of possibilities relative to the three previous emissions scenarios (B1-low, A1B-medium and A2-high) presented by Australian Bureau of Meteorology and CSIRO (2011) (Figure 1.2). The higher Special Report on Emission Scenarios (SRES) scenario (A1FI) not used by the Australian Bureau of Meteorology and CSIRO (2011) is also shown on the plot. All scenarios are plausible future pathways relevant to climate adaptation policymakers and planners. The lowest scenario shows the likely outcome of reducing

emissions (mitigation), and the highest scenario shows the impact of 'a pathway with no climate policy and high emissions'. Recent carbon dioxide (CO_2) emissions have been tracking the highest scenario (Peters et al., 2013).

Multiple Possible Futures

As it is not possible to identify a single 'best' GCM, nor a single scenario that will best approximate future emissions, it is not prudent to rely on a single projected 'future climate'. The Pacific Climate Futures web-tool www.pacificclimatefutures.net/ provides guidance on the range of different future climates for different countries, years and emissions scenarios. Climate futures beyond the range of RCP scenarios and those simulated by the 26 climate models analysed in this report are also possible. While, climate

futures beyond 2100 are not considered here, warming will continue beyond 2100 under all RCP scenarios except RCP2.6. It is virtually certain that global mean sea level will continue beyond 2100, with sea-level rise due to thermal expansion to continue for many centuries.

Natural Variability

When interpreting projected changes in the mean climate in the Pacific, it is important to keep in mind that natural climate variability, such as the state of the ENSO, strongly affects the climate from one year to the next, and the Interdecadal Pacific Oscillation (IPO) can affect the climate from one decade to the next. For example, within a warming trend it is still possible in some locations to experience years with mild temperatures, although these would become less frequent over time.
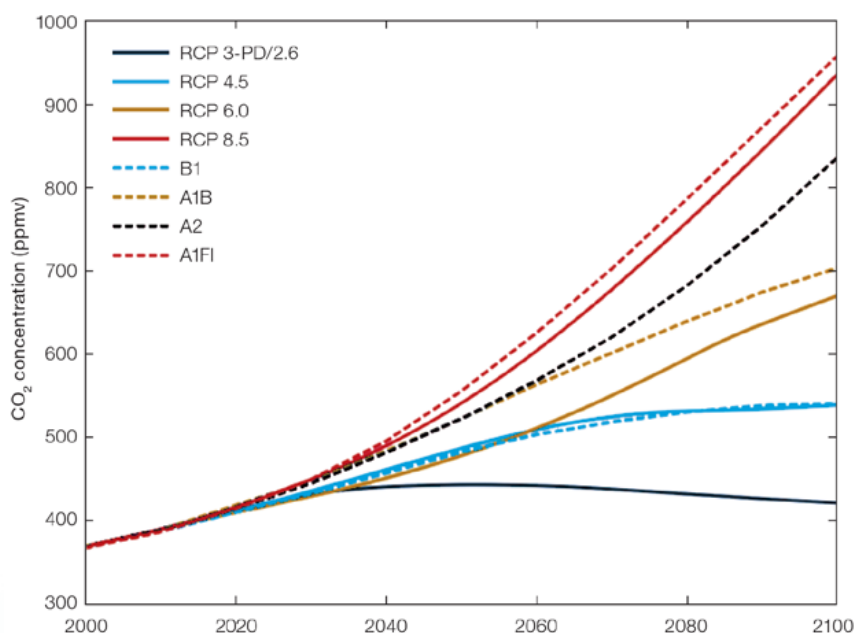

Figure 1.2: Comparison of CO_2 concentrations in parts per million by volume (ppmv) for CMIP3 (SRES, dotted lines) and CMIP5 (RCP, solid lines) emissions scenarios.

Confidence statements

Confidence statements are a characterisation of uncertainty and an estimation of the level of confidence in the projections based on expert judgment. They are generated in the same way as for the report by Australian Bureau of Meteorology and CSIRO (2011). Greater confidence is placed in a result if the driving mechanism is understood, when models have low biases in their simulation of the processes involved, and there is high model agreement on the projected change (Australian Bureau of Meteorology and CSIRO, 2011, Volume 2, Chapter 1.7).

A confidence rating for the direction of change is given in some sections of the country chapters, and confidence ratings for the magnitude of change are given in the summary table. Confidence in the magnitude of change is how well the multi-model mean is judged to represent the expected change for a particular scenario. Confidence in the magnitude

of change is often lower than for direction of change, and is reduced when there are model biases in relevant climate features and where there is a wide range of projections from the models.

Some confidence statements have changed from Australian Bureau of Meteorology and CSIRO (2011), including some rainfall confidence ratings reduced from *high* to *medium* or from *medium* to *low*. This is primarily due to new research showing greater uncertainty in the projection of large-scale climate features and processes in the western tropical Pacific (updated findings on climate features are summarised in Box 1) and also a greater range of projections in CMIP5 compared to CMIP3 models. Some of the patterns of change previously thought to predominate have now been found to be less important. We have developed further understanding of the various processes driving change in the western tropical Pacific, and revised some previously simple viewpoints. In some cases this more

sophisticated understanding leads to a reduction in confidence ratings. For example, we now know that the simple 'wet get wetter and the dry get drier' pattern of change does not predominate over the western tropical Pacific, but there are other important drivers of change such as increases of sea-surface temperature gradients near the equator leading to increased rainfall (Chadwick et al., 2013).

Many CMIP5 models retain the 'cold-tongue bias' that was present in most CMIP3 models (Grose et al., 2014). This means that models have a region along the equatorial Pacific where the sea-surface temperatures are colder than the observations, and rainfall is less than in observations. This is reflected in an incorrect shape of the edge to the West Pacific Warm Pool, and is linked to biases in the large-scale climate features in the western tropical Pacific, such as the SPCZ (Figure 1.3 and Box 1). This bias is the largest factor reducing the confidence rating for projections in many Partner Countries.
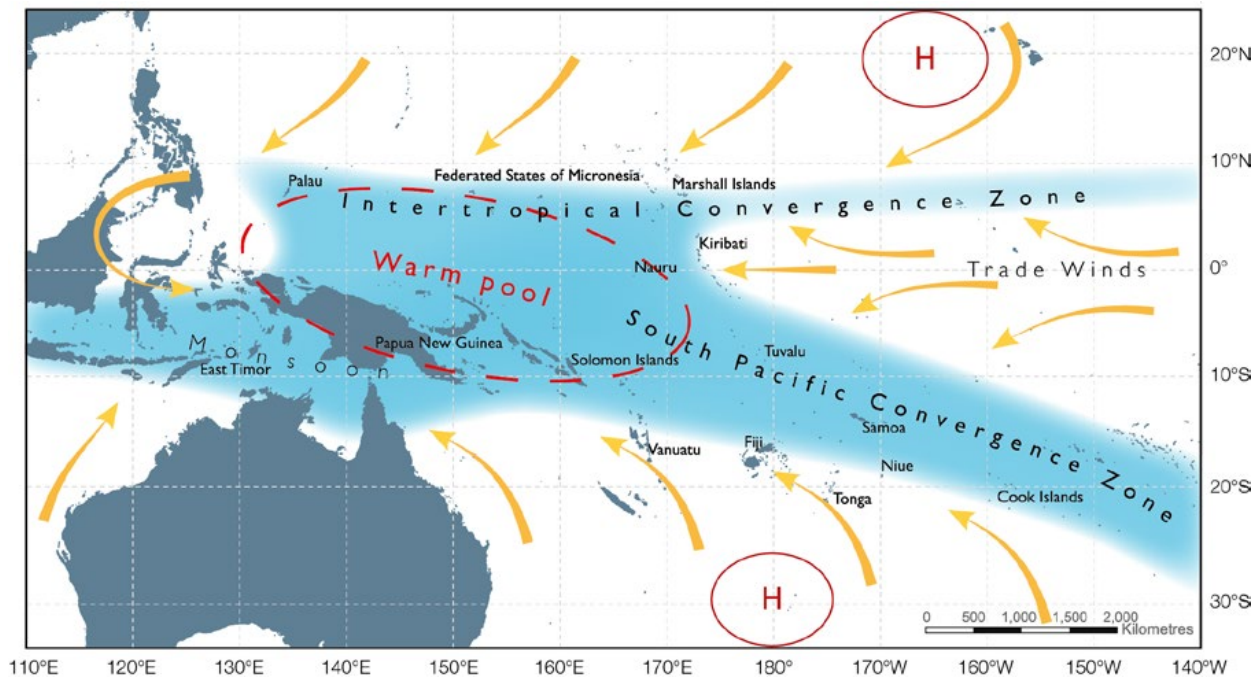

Figure 1.3: Map showing the average positions of the major climate features of the western tropical Pacific region in November to April. The yellow arrows show near surface winds, the blue shading represents the bands of rainfall (convergence zones with relatively low pressure), and the red dashed oval indicates the West Pacific Warm Pool. H represents the typical positions of moving high pressure systems.

Box 1: Projected changes in large-scale climate features in the western tropical Pacific

There are two main processes that determine changes in the West Pacific Monsoon, Inter-Tropical Convergence Zone and South Pacific Convergence Zone : (i) in a warmer climate, atmospheric moisture is increased, leading to increased rainfall ('thermodynamic' processes), and (ii) changes in atmospheric circulation, such as weaker surface wind convergence, lead to decreased rainfall in some regions ('dynamic' processes). The balance between these two processes is different for each location and in each climate model, leading to a wide range of projections for rainfall in some cases.

El Niño–Southern Oscillation (ENSO): As for the previous CMIP3 models reported in Australian Bureau of Meteorology and CSIRO (2011), there is no consensus from the new CMIP5 models on whether El Niño and La Niña events will become more or less frequent, or whether El Niño-driven sea-surface temperature variability will become stronger or weaker in a future warmer climate. However, recent research shows the frequency of extreme El Niños is expected to double due to climate change, with the average frequency increasing from once every 20 years to once per decade (Cai et al., 2014). All models indicate that El Niño and La Niña events will continue to occur and have a significant impact on interannual variability in the region. Some of the impacts of ENSO on rainfall (e.g. floods) may intensify in a warmer climate due to increased atmospheric moisture (e.g. Seager et al., 2012). Global warming is also expected to enhance average rainfall along the equator, and new research suggests it will also enhance El Niño-driven drying in the western tropical Pacific and El Niño-driven increases in rainfall over the central and eastern tropical Pacific (Power et al., 2013).

South Pacific Convergence Zone (SPCZ): The average December–February position of the SPCZ is not expected to change significantly (Brown et al., 2013a), although years when the SPCZ moves north and merges with the ITCZ (zonal SPCZ events) are projected to become more frequent (Cai et el., 2012). Changes in SPCZ rainfall are uncertain due to the balance between thermodynamic and dynamic processes (Widlansky et al., 2013; Brown et al., 2013a). Changes are also sensitive to sea-surface temperature gradients, which are not well simulated by many models (Widlansky et al., 2013).

Inter-Tropical Convergence Zone (ITCZ): Climate models indicate that rainfall in the ITCZ will increase, particularly in the June–August period, amplifying the seasonal cycle. The area of the ITCZ is projected to expand as rainfall increases on the equatorward side of the ITCZ. CMIP3 models show a small southward shift (less than 1° latitude) in the average position of the ITCZ in March–August (Australian Bureau of Meteorology and CSIRO, 2011, Volume 1 Chapter 6.4.3). The results from CMIP5 models (this report) are similar.

West Pacific Monsoon (WPM): CMIP3 models show evidence of a slight weakening of westerly winds in the equatorial WPM region in a warmer climate (Smith et al., 2012). Despite this, most models show increases in monsoon rainfall in a future warmer climate, with much of the increase occurring during the wet season, leading to an amplification of the seasonal cycle (Australian Bureau of Meteorology and CSIRO, 2011, Volume 1 Chapter 6.4.4). The results from CMIP5 models are similar (Brown et al., 2013b); see also this report.

1.5.2 Presentation of Projections

The country reports provide a summary of GCM results, including a detailed description of the projections and an explanation of the important model biases. Projections are given for average surface air temperature and rainfall, and extremes (daily minimum and maximum air temperatures, daily rainfalls,12-month drought and tropical cyclones) for each of the four RCPs (2.6, 4.5, 6 and 8.5) and four 20-year time periods centred on 2030, 2050, 2070 and 2090. Projections for ocean acidification, coral bleaching, sea-level rise and wind-driven waves are provided, followed by a table summarising the projections, including ranges of change in selected climate variables.

Surface air temperatures in the Pacific are closely related to sea-surface temperatures (SST), so the projected changes to air temperature given in the projections summary tables can be used as a guide to the expected changes to SST. The availability of data for each RCP depends on the climate variable in question (Appendix A).

CMIP5 GCMs have relatively coarse spatial resolution (around 100–300 km between data-points), meaning there may be considerable deviation from these large-scale projections at smaller scales due to island topography and other local features. A technique known as dynamical downscaling has been used to enhance the representation of these influences. This requires high resolution atmospheric model simulations, driven by changes in SSTs simulated by a subset of CMIP3 GCMs. Dynamical downscaling results are only discussed in the presentation of projections for each Partner Country when they highlight small-scale details not present in the GCM projections. Dynamical downscaling provides more detail at the local level, but this does not guarantee increased reliability in representing the future climate. Since downscaling is computationally demanding, a subset of GCMs is

usually downscaled, so the range of downscaled projections does not cover the full range of uncertainty from GCMs. It is not good practice therefore to assume that projections based on a small number of downscaled models are necessarily more reliable than projections from a larger number of (coarser) models. In general, the projections provided for each Partner Country are not specific to any town or city. Instead, they refer to an average change over the broad geographic region encompassing the country of interest and the surrounding ocean, with four countries being divided into nominal sub-regions (Cook Islands, Federated States of Micronesia, Kiribati and Marshall Islands) due to the differing influences of large-scale climate features across those countries (Figure 1.3).

Figures displaying projections show an observed dataset up to the year 2006, and projections from 2005 onwards. For simplicity, data from a single observational dataset are shown over the observational period of each projection figure; the GISS-TEMP (Goddard Institute for Space Studies surface temperature analysis) dataset for air temperature (Hansen et al., 2010), the HadISST dataset for sea-surface temperature (Rayner et al., 2003) and the Global Precipitation Climatology Project (GPCP) dataset for rainfall (Adler et al., 2003). Each of the gridded datasets uses its own specific method for converting sparse, irregularly spaced and temporally incomplete observations into a gridded product. Some differences may therefore be evident in the year to year values, and long-term trends from these products compared to station records or other gridded datasets. There are also some inevitable differences between measurements at a single station and the areal average from gridded datasets. We therefore use the average over the country

and surrounding ocean from gridded datasets to ensure comparability with model outputs.

Approach to Presenting the Projections

The following approach for the direction and magnitude of change has been used for projections of surface air temperature, sea-surface temperature (SST), rainfall, extreme weather events, ocean acidification and sea level throughout the report.

Projected Direction of Change

Each climate variable has a statement for the likely direction of change over the course of the 21st century. This likely direction of change is estimated from various lines of evidence, including physical theory and principles, process-based studies of the relevant large-scale climate features (Box 1) and the range of model projections for all scenarios. The statement is followed by a confidence level, which is assigned through assessing the range of evidence and the agreement between these lines of evidence.

Projected Magnitude of Change

For each climate variable, a statement is provided for the level of confidence in the simulated magnitude of change (quantified in the Summary Table(s) at the end of each chapter). For example, for RCP8.5 the models may simulate a change in (multi-model mean) annual rainfall of +4% (range: -4–+9%) by 2030, +12% (-14–+24%) by 2090 and +12% (-14–+24%) by 2090 (compared with the observed rainfall for the period 1986–2005). The confidence in the magnitude of change defines how well we think the multi-model mean value represents the most likely projection. The confidence level is supported by one or more statements based on expert judgement about the ability of the models to capture the full range

of possible futures. A very large range between model results also reduces the confidence in the multi-model mean magnitude of change. The confidence associated with the magnitude of change need not be the same as that for the projected direction of change. For example, if expert judgement of theory, relevant processes and models suggests that a projected increase in rainfall is most likely, confidence in the direction of change might be *high*. However, if the models are known to systematically underestimate rainfall in the country of interest, then confidence in the magnitude of change might be *low*.

1.5.3 Detailed Projection Methods

The methods used to generate projections are the same as for Australian Bureau of Meteorology and CSIRO (2011), except where otherwise further described for each variable.

Mean Temperature and Rainfall

In the figures and summary table for each country report, the range between CMIP5 models is presented as the lowest 5% and the highest 95% value across models. With around 25 models used, this means in most cases the highest and lowest model values are not included in the plotted lines or calculated values, and the range shows the second highest and second lowest values. This is consistent with the IPCC (2013) method, but slightly different to the use of two standard deviations from the mean in Australian Bureau of Meteorology and CSIRO (2011). Also, the 5% and 95% range of models are shown as values in the table rather than as a single value of two standard deviations (with the ± symbol) used by the Australian Bureau of Meteorology and CSIRO (2011).

Extreme Daily Temperature and Rainfall

Projected changes in days of extreme temperature and rainfall were made relative to the event that occurred, on average, once every 20 years, calculated for the period 1986–2005. This 1-in-20-year event was calculated using the method of L-moments to fit the Generalised Extreme Value distribution to annual maxima series. A boot-strapped Kolmogorov-Smirnov goodness-of-fit test was applied to test the suitability of the fitting method, similar to that performed by Kharin and Zwiers, (2000). In general, two types of projection are given:

- Change in the magnitude of the 1-in-20-year event obtained by comparing fitted distributions of the future periods with the present. For example, in a warming climate the temperature experienced on the 1-in-20-year hot day may increase by 2.0°C by 2090 (i.e. 2080–2099) relative to 1995 (i.e. 1986–2005).

- Change in the frequency of the present day 1-in-20-year event obtained by inverting the distribution for the future period for the present day return value. For example, in a climate of increasing rainfall, the current (i.e. 1986–2005) 1-in-20-year daily rainfall total may become on average a 1-in 12-year event by 2090 (i.e. 2080–2099).

Drought

Projected changes in the frequency and duration of mild, moderate, severe and extreme meteorological droughts were made using the Standardized Precipitation Index (SPI) (Australian Bureau of Meteorology and CSIRO, 2011, Volume 1, Chapter 6.2.7.3; Lloyd-Hughes and Saunders, 2002). This index is based solely on rainfall (i.e. periods of low rainfall are classified as drought). It does not take into account factors such as evapotranspiration or soil moisture content. The SPI is commonly used in many regions including the Pacific due to the relative simplicity with which it is calculated, as well as its relevance across temporal and spatial scales.

To calculate the SPI, the monthly time series of rainfall must be accumulated using a moving window, according to the type of drought of interest. The 12 month SPI is calculated in this report.

For each month of the year, an assumed distribution is fitted to a representative sample of the accumulated (or 'smoothed') time series of rainfall. A two-parameter gamma distribution is assumed, with the period of fitting applied for each model from 1900 to 2005. Every month in the accumulated series is then assigned a percentile score according to the appropriate fitted gamma-distribution for that particular month. This percentile score can then be transformed into a standardised z-score (i.e. SPI score) by applying a simple transformation from the cumulative distribution (gamma) to a normal distribution (Lloyd-Hughes and Saunders, 2002).

The drought categories (McKee et al., 1993) according to the SPI score are as follows:

SPI value	Drought category
0–-0.99	Mild drought
-1–-1.49	Moderate drought
-1.5–-1.99	Severe drought
-2 or less	Extreme drought

A drought event is defined as a period where the SPI is continuously negative and reaches a value of -1.0 or less (McKee et al., 1993). The drought duration is defined by the zero-crossings bounding a drought event, i.e. it begins when the SPI falls below zero and ends where the SPI becomes positive, following an SPI value of -1.0 or less (Figure 1.4).

The method of defining drought conditions differs slightly from the Australian Bureau of Meteorology and CSIRO, 2011, Volume 1, Section 6.2.7.3. A drought event was previously defined as a peak bounded by a particular threshold. For example, an extreme drought length was counted as only the months with an SPI of below -2, and not including the preceding and following months that were still in drought.

The overall change in the incidence of drought is described by the 'percent of time in drought'. This is calculated by aggregating the durations for drought events in the moderate, severe and extreme categories during the time period of interest. Projections of drought in each category for drought duration and frequency were estimated according to the median of model projections for each scenario for each period. Confidence in drought projections is informed by the model projection spread, as well as the confidence in rainfall projections.
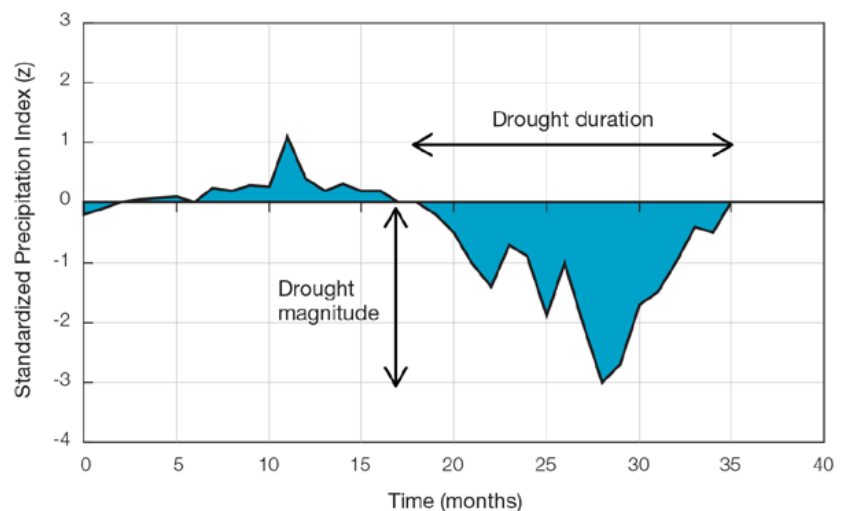

Figure 1.4: A schematic diagram showing how a drought event is defined using the Standardized Precipitation Index.

Tropical Cyclones

The current generation of GCMs is able to simulate the broad-scale atmospheric conditions associated with tropical cyclone activity, but they have insufficient temporal and spatial resolution to capture the high wind speeds and other small-scale features associated with observed tropical cyclones. Despite this limitation, GCMs do produce atmospheric circulations that resemble tropical cyclones with global distributions that generally match the observed tropical cyclone climatology.

The projected changes of tropical cyclone frequency and location were derived using the following methods:

Three 'empirical methods' that infer tropical cyclone activity from the large-scale climatological environmental conditions were applied to the outputs of 17 CMIP5 GCMs. These schemes are known as the Genesis Potential Index (Emanuel and Nolan, 2004), the Murakami modification of the Genesis Potential Index (Murakami and Wang, 2010) and the Tippett Index (Tippett) (Tippett et al., 2011).

Two 'direct detection' schemes were applied to the outputs from a subset of CMIP5 GCM model outputs: the CSIRO Direct Detection (CDD) scheme (Nguyen and Walsh, 2001; Hart, 2003) and the Okubo-Weiss-Zeta Parameter (OWZP) (Tory et al., 2013 a,b,c).

The CDD identifies features that have the characteristics of a tropical cyclone, i.e. a closed low pressure system accompanied by strong winds and a warm core through the depth of the atmosphere. The CDD uses a wind speed threshold set at 70% of the value recommended by Walsh et al. (2007) and was applied to outputs from a subset of 17 CMIP5 GCMs for which suitable sub-daily, multi-level model outputs were available. Of the 17 CMIP5 models examined, the tropical cyclone detections in 11 models reproduced a current-climate tropical cyclone climatology with annual tropical cyclone numbers

within ±50% of observed. The OWZP identifies larger-scale weather features that are present while tropical cyclones form, e.g. a persistent region of circular flow and high humidity. The OWZP has been applied to 14 CMIP5 GCMs for which suitable daily, multi-level model outputs were available. Of these models, the tropical cyclone detections in nine models reproduced a current-climate tropical cyclone climatology with annual tropical cyclone numbers within ±50% of observed.

The results were compared with the findings documented in Australian Bureau of Meteorology and CSIRO (2011) and provide new projected changes in the frequency of tropical cyclones at the end of the 21st century under RCP8.5. The cyclonic wind hazard for both the current and future climate was also assessed using Geoscience Australia's Tropical Cyclone Risk Model (TCRM).

Tropical Cyclone Wind Hazard

The current climate wind hazard associated with tropical cyclone activity in the western tropical Pacific was estimated by applying the TCRM to the historical track record. The TCRM is a statistical-parametric model of tropical cyclone behaviour which enables users to generate synthetic records of tropical cyclones representing many thousands of years of activity. The model was applied to tracks of tropical cyclone-like vortices detected in the CMIP5 GCM outputs (using the CDD scheme) to determine how the cyclonic wind hazard may change in the future. The TCRM uses an auto-regressive model, similar to the model developed by Hall and Jewson (2007), to create synthetic tracks of tropical cyclone events based on the characteristics (speed, intensity, bearing, size and genesis location) of a record of tropical cyclone events. Once a set of synthetic tropical cyclone events has been created, a parametric wind field (Powell et al., 2005) and boundary layer model (Kepert, 2001) is applied to each track, and the maximum wind speed over the life of

each event is captured. A generalised extreme value distribution is then fitted to the maximum wind speed values for each location (Hosking, 1990).

Ocean Acidification

The figures in each country report show how distributions of aragonite saturation change between the year 2000 and 2099. Aragonite is a metastable form of calcium carbonate used by hard reef building corals to build skeletons. As the oceans acidify in response to increasing ocean carbon uptake, the carbonate ion concentration of seawater decreases making it harder for corals to build these skeletons. Saturation states above 4 are optimal, 3.5-4 adequate, and between 3-3.5 marginal, with no corals historically found below 3 (Guinotte et al., 2003). The transition from adequate to marginal conditions (aragonite saturation state of 3.5) is labelled in the projection figures provided in each country report. By aggregating the data, the plotted distribution includes the interannual variability within each model and the variation between models. The graphs show the median value, the interquartile range, and the 5th and 95th percentiles.

This method differs from that described previously by the Australian Bureau of Meteorology and CSIRO (2011), in which climate models without a carbon cycle were used. Projections from coupled climate-carbon models that include an active carbon cycle under three of the RCPs (2.6, 4.5 and 8.5) are used in the new simulations, which allow the changes in the ocean carbon cycle to be projected, and their impact on ocean acidification quantified. Coupled climate-carbon models presently simulate a larger range of values compared to the observed aragonite saturation state in the western tropical Pacific. These biases were removed by scaling the mean value of aragonite in the year 2000 to match the observed values reported in Kuchinke et al. (2014).

As coupled carbon-climate models do not explicitly simulate coral reefs and the key ecosystem services they provide, the changes in aragonite saturation can only be quantified for the open ocean. While increasing ocean acidification is a significant stressor in the western tropical Pacific, it remains only one of a number of stressors facing coral reefs in the future, e.g. coral bleaching, storm damage, fishing pressure and other human impacts.

Coral Bleaching Risk

Coral bleaching risk is increased by elevated water temperatures. When ocean temperatures exceed summertime maximums by 1.0–2.0°C for a prolonged period (1–3 weeks), the corals become stressed, raising the risk of coral bleaching {Berkelmans et al., 2004; Hoegh-Guldberg, 1999). The longer the temperature is elevated above this limit, the greater the coral bleaching risk. The risk therefore depends on the duration and magnitude of elevated temperature. Degree Heating Weeks (DHW), defined as the sum of weekly sea-surface temperature (SST) anomalies above the thermal stress threshold accumulated over 12 weeks (Donner, 2009), is a measure of this accumulation of stress. DHW values above 8 means that the risk of bleaching is considered severe, e.g. eight weeks at 1.0°C above the thermal limit. Despite the severe risk, this does not mean that coral bleaching will occur, only that it is likely. When bleaching occurs, recovery is dependent on the severity and extent of the bleaching event.

One impact of long-term ocean warming will be a decrease of the time between two risk events, defined as the frequency (or recurrence) and duration of severe bleaching risk events. Once the frequency of severe bleaching events occurs more often than once every five years, the long-term viability of coral reef ecosystems becomes threatened (Donner, 2009).

Ocean warming will increase the duration and recurrence of severe bleaching risk. As projected changes in SST show a large range across RCPs and climate models, changes in the recurrence and duration of severe bleaching risk are presented for different projected SST changes. The occurrence of elevated SSTs (above the thermal threshold) is also dependent on ENSO frequency and amplitude. As there is little consensus on how ENSO frequency and amplitude may change in the future (See Box 1, Section 1.5.1 in this report), the observed SST variability (1982–2012) is used for the calculation of the projected coral bleaching risk, assuming no change in ENSO behaviour.

Analysis in the country reports only represents coral bleaching due to projected changes of open ocean SST, and does not take into account other factors that could influence coral bleaching, such as:

- Temperature changes at the reef scale, which can play a role in modulating large-scale changes;
- Stressors like ocean acidification, storm damage, fishing pressure and

other human impacts, which may limit the ability of coral reefs to cope with elevated temperature, resulting in lower thermal thresholds above which corals become stressed and prone to bleaching; and
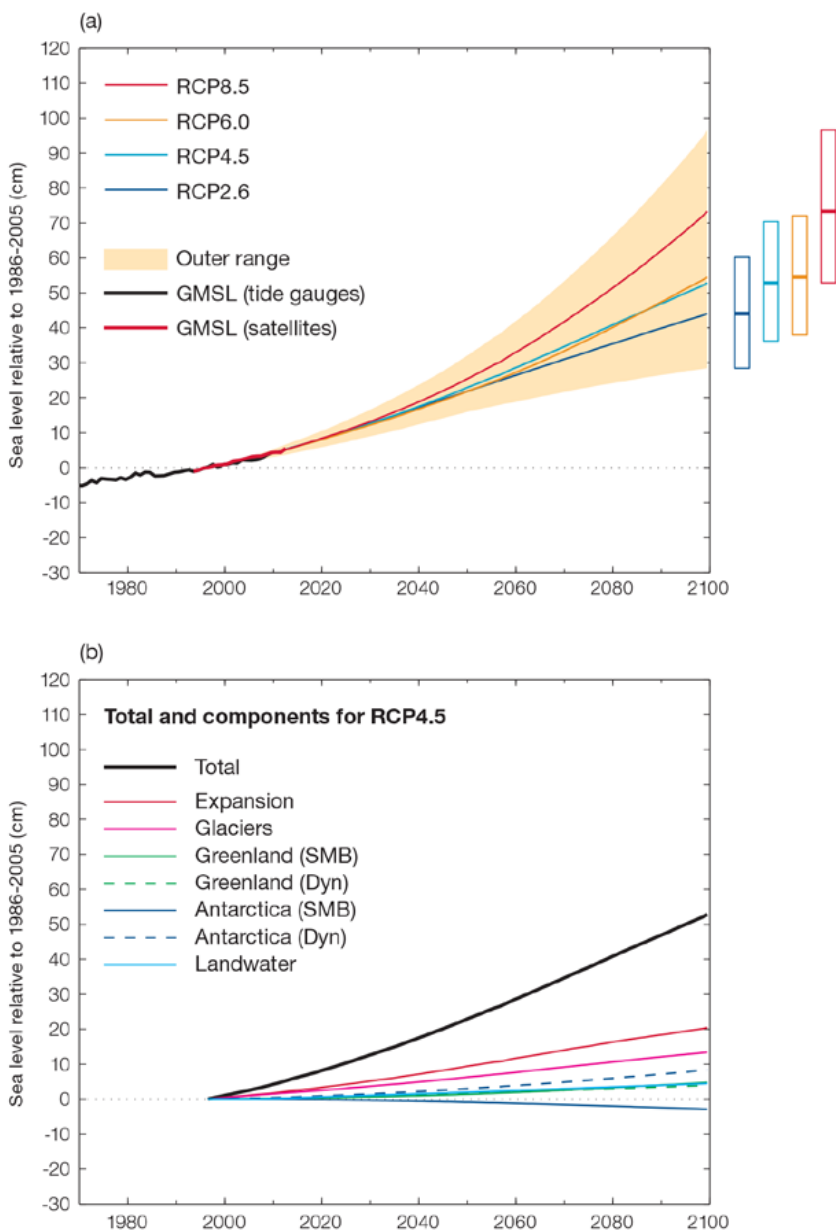
- The risk of coral bleaching decreasing due to coral adaptation to higher temperature (acclimatization or shift in communities).

Sea level

Projections of global meal sea-level rise require consideration of ocean thermal expansion, the melting of glaciers and ice caps, the surface mass balance (SMB) and dynamic response of the ice sheets of Antarctica and Greenland, and any changes in land water storage. The IPCC (2013) includes projections of global mean sea-level rise and various contributions under four different RCPs (Table 1.3 and Figure 1.5). The projected likely ranges between the periods 1986–2005 and 2081–2100 are from 26 to 55 cm for the RCP2.6 emissions scenario and from 45 to 82 cm for the RCP8.5 emissions scenario.

Table 1.3: Median values and likely ranges (5th to 95th percentiles) in metres for projections of global average sea-level rise and its components in 2081–2100 relative to 1986–2005 under four emission scenarios (modified from Table 13.5 of the IPCC (2013).

	RCP2.6	RCP4.5	RCP6.0	RCP8.5
Thermal expansion	0.14 [0.10–0.18]	0.19 [0.14–0.23]	0.19 [0.15–0.24]	0.27 [0.21–0.33]
Glaciers	0.10 [0.04–0.16]	0.12 [0.06–0.19]	0.12 [0.06–0.19]	0.16 [0.09–0.23]
Greenland Ice Sheet SMB	0.03 [0.01–0.07]	0.04 [0.01–0.09]	0.04 [0.01–0.09]	0.07 [0.03–0.16]
Antarctic Ice Sheet SMB	-0.02 [-0.04–-0.00]	-0.02 [-0.05–-0.01]	-0.02 [-0.05–-0.01]	-0.04 [-0.07–-0.01]
Greenland Ice Sheet Rapid Dynamics	0.04 [0.01–0.06]	0.04 [0.01–0.06]	0.04 [0.01–0.06]	0.05 [0.02–0.07]
Antarctic Ice Sheet Rapid Dynamics	0.07 [-0.01–0.16]	0.07 [-0.01–0.16]	0.07 [-0.01–0.16]	0.07 [-0.01–0.16]
Land Water Storage	0.04 [-0.01–0.09]	0.04 [-0.01–0.09]	0.04 [-0.01–0.09]	0.04 [-0.01–0.09]
Sea Level Rise in 2081–2100	0.40 [0.26–0.55]	0.47 [0.32–0.63]	0.48 [0.33–0.63]	0.63 [0.45–0.82]

Figure 1.5: (a): Projections of global mean sea-level rise (GMSL) for four emission scenarios relative to 1986–2005. Bars on the right indicate likely ranges (5–95%) and the median values of global sea-level rise in 2100.

(b) Projections of (total) global mean sea-level rise and its components (from 1995) to 2100 for the RCP4.5 emissions scenario. Refer to Table 1.3 for list of components.
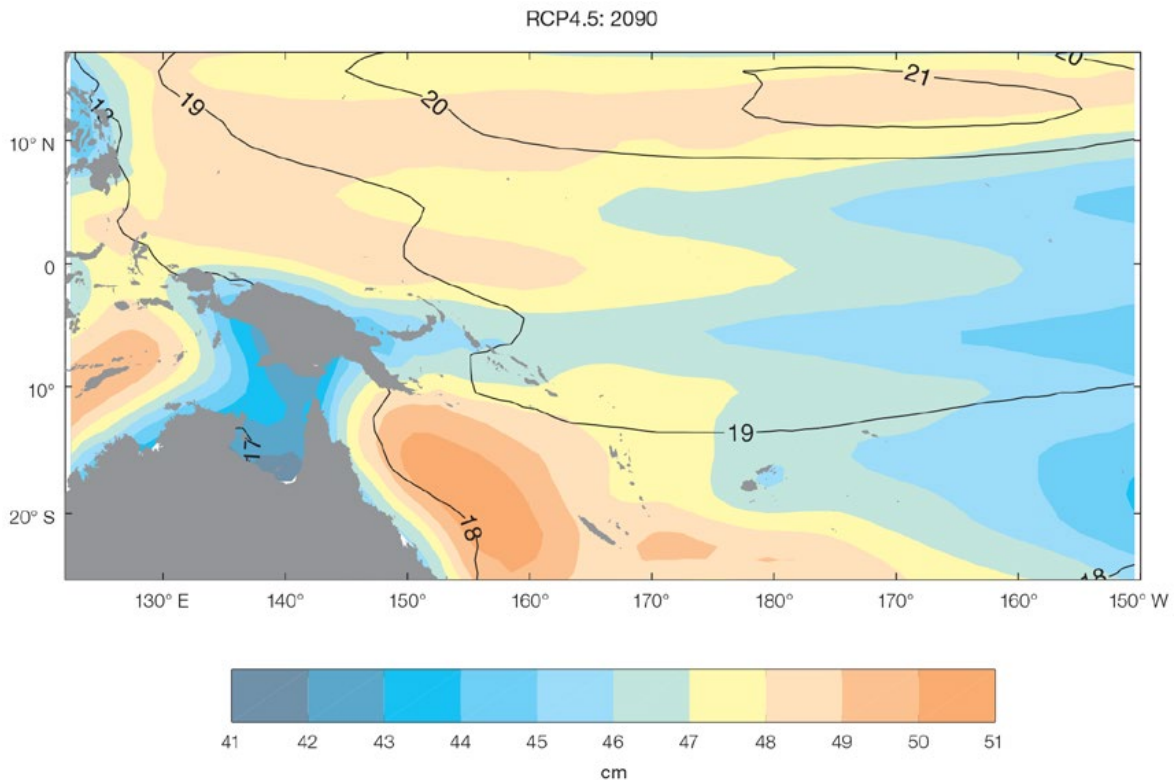
To estimate regional sea-level changes in the western tropical Pacific, the approach of Church et al. (2011) and Slangen et al. (2012) was used to combine global average sea-level projection and regional distributions associated with ocean density and circulation changes, and redistributions of mass due to changes in ice sheets, glaciers and ice caps. Each of the terms associated with a change in mass to the ocean implies changes in the Earth's gravitational field and vertical movement of the crust (sea-level fingerprints). The analysis for the country reports used the fingerprints calculated by Mitrovica et al. (2011). Additionally, an estimate was included of land motions associated with an ongoing glacial isostatic adjustment associated with changes in surface loading over the last glacial cycle (Mitrovica et al., 2011). The glacial isostatic motions are relatively small for the western tropical Pacific.

There are regional variations in projected sea-level changes for 2081–2100 relative to 1986–2005 for each emissions scenario. An example for the RCP4.5 scenario is shown in Figure 1.6. The amount of regional sea-level rise is largest for the RCP8.5 and smallest for the RCP2.6 emissions scenario, with RCP4.5 and RCP6.0 being similar (not shown). Compared with the Australian Bureau of Meteorology and CSIRO (2011) and based on Meehl et al. (2007) and CMIP3 models, the updated country reports give larger central projections of sea-level rise for comparable emissions scenarios, but with (1.0–4.0 cm) smaller uncertainty ranges.

RCP4.5: 2090

Figure 1.6: The regional distribution of projected sea-level rise for the period 2081–2100 relative to 1986–2005 from emissions scenario RCP4.5. The uncertainty is indicated by the contours (in centimetres).

The increase of projected sea-level rise is mainly due to larger contributions from glacier and ice caps, and combined Greenland and Antarctica ice sheets (both SMB and dynamics). Another contributing factor which is not mentioned in Australian Bureau of Meteorology and CSIRO (2011) is a positive contribution from ground water depletion and reservoir storage. The slightly smaller uncertainty ranges in the updated country reports can be partially explained by better agreement of regional sea level simulation among CMIP5 models than for CMIP3 models.

Wind-driven Waves

Projections of future wave climates were made in a similar manner to the hindcast, using 3-hourly surface wind data from four selected CMIP5 GCMs to drive the WAVEWATCH III wave model (Tolman, 1991, 2009) on a 1 degree grid between -80˚S and 80˚N. All models had substantial bias in wave parameters compared to reanalysis data. The four models were chosen on the basis of relatively high spatial resolution and early availability of high temporal resolution (3-hourly) data. The models' monthly surface winds were compared to the full distribution of CMIP5 GCM winds,

and it was found that all four fall in the middle 50% of projected winds. These models are therefore considered to be typical of other CMIP5 models, and it is assumed in the analysis for the updated country reports that they represent the distribution of the full model ensemble. In practice they do not, so uncertainty estimates provided are likely to underestimate the model uncertainty in the full CMIP5 ensemble.

Projections were made for RCP4.5 and RCP8.5 over two 20-year periods (2026–2045 and 2081–2100), relative to a 1986–2005 historical period.
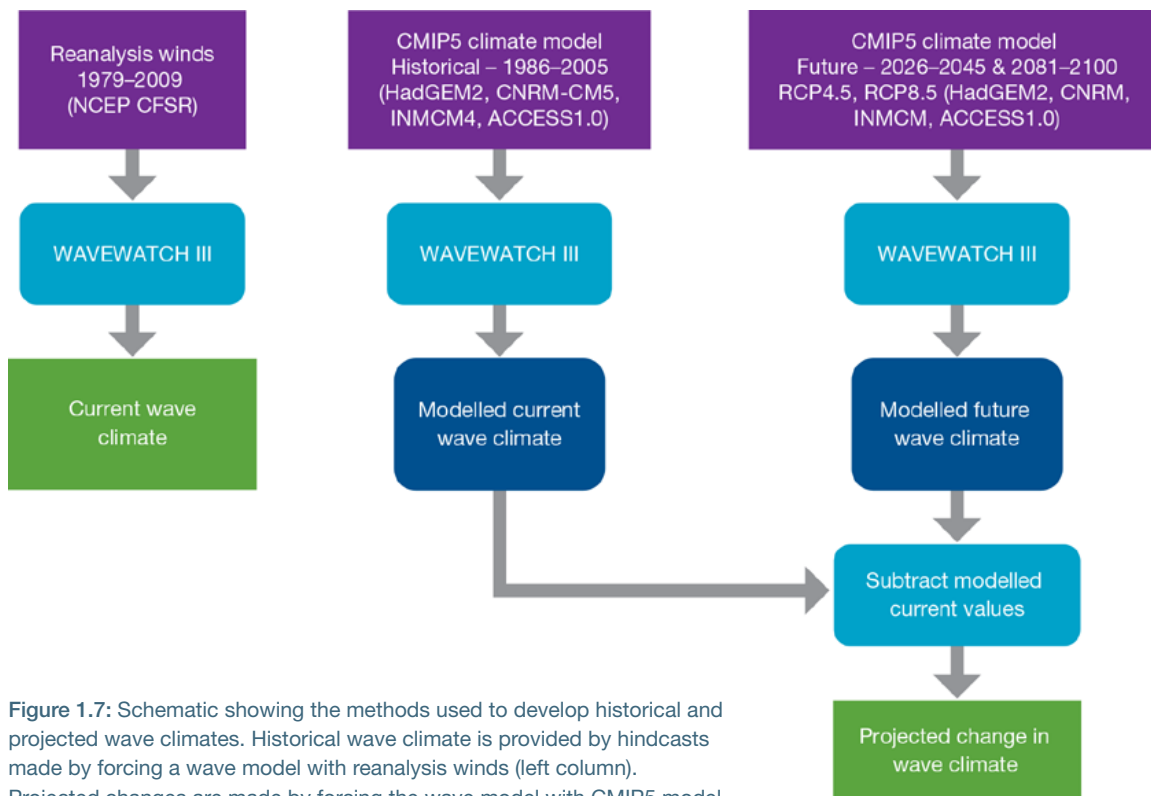
Figure 1.7: Schematic showing the methods used to develop historical and projected wave climates. Historical wave climate is provided by hindcasts made by forcing a wave model with reanalysis winds (left column). Projected changes are made by forcing the wave model with CMIP5 model winds (middle column). Changes in wave properties are found by the difference between the historical and future time slices (right column).

The projected changes in wind-wave climate are the ensemble average of changes between each model's future scenario and its historical values. Thus the hindcast was used to describe the historical wave climate, but the historical model ensemble was used as the benchmark for projections (Figure 1.7). Both sets of historical values are provided (Seasonal Cycles) for comparison of model bias from the more accurate hindcast values.

The bias in wave properties between the models and the reference dataset is typically much larger than the changes between the historical and projection runs, which combined with the uncertainty of ENSO index projections means that all wave projections have low confidence ratings (Hemer et al., 2013).

Due to the coarser spatial resolution of the CMIP5 models, a set of values over a grid covering the area of most countries was extracted and averaged at each time step to make

regional projections, rather than using the values from the nearest model grid point to the locations of interest used in the hindcast. This is done for consistency with other projection variables.

Data Presented

To provide future projections, the difference between all four models' historical and future cases was calculated for each month of the year and averaged across the four models. Projected change in wave height was calculated for each month and plotted, similar to the observations section, while seasonal projected change values and confidence ranges are given for all three variables (height, period and mean direction).

The ensemble mean projected change in wave height is plotted, with a box showing the standard deviation between the four models' means in each month. This is a very small sample so is likely to be an

underestimate of the full range of CMIP5 model means. The 5–95% whisker range was estimated by calculating 1.64 times the standard deviation of the model means assuming a normal distribution. The same method was used in the projection tables to generate 5–95% confidence ranges, but taking the differences over four months (December–March and June–September) for the four models, and calculating the standard deviation of these 16 values rather than four in any one month.

Projection Summaries

A summary table of projections is included at the end of each chapter. In some cases there are two or three tables for different country regions that span a wide geographical area, and imperial units are included for the Federated States of Micronesia, the Marshall Islands and Palau.